



Biosynthesis of La_2O_3 Nanoparticles using *Lawsonia inermis* Leaf Extract

P. Subramanian^a and S. Alwin David^{b+++}

^a Department of Educational Planning and Administration, Tamil Nadu Teachers Education University, Chennai – 97, Tamil Nadu, India.

^b Department of Chemistry, V. O. Chidambaram College, Tuticorin – 628008, Manonmaniam Sundaranar University, Abishekapatti, Tirunelveli - 627 012, Tamil Nadu, India.

Authors' contributions

This work was carried out in collaboration between both authors. Both authors read and approved the final manuscript.

Article Information

DOI: <https://doi.org/10.56557/upjoz/2024/v45i184434>

Open Peer Review History:

This journal follows the Advanced Open Peer Review policy. Identity of the Reviewers, Editor(s) and additional Reviewers, peer review comments, different versions of the manuscript, comments of the editors, etc are available here: <https://prh.mbimph.com/review-history/3970>

Original Research Article

Received: 27/06/2024

Accepted: 30/08/2024

Published: 03/09/2024

ABSTRACT

The article explains the biogenesis of lanthanum oxide nanoparticles (La_2O_3 NPs) utilizing *Lawsonia inermis* extract as an easy, safe, and efficient approach. The La_2O_3 NPs were synthesized by reducing $\text{La}(\text{NO}_3)_3 \cdot 6\text{H}_2\text{O}$ with *Lawsonia inermis* leaf extract as a reducing agent. Fourier-transform infrared spectra were used to determine how the biomolecules in the *Lawsonia inermis* leaf extract contributed to the synthesis of La_2O_3 NPs. The UV-visible spectrum of the biosynthesized La_2O_3 NPs revealed absorption peaks at the La_2O_3 NPs' absorption maxima, which is 245 nm. As per the scanning electron microscopy investigation, the biosynthesized La_2O_3 nanoparticles (NPs) with a size of 30 to 60 nm had an uneven shape. EDAX confirmed that La and O were present in the La_2O_3 NPs. La_2O_3 NPs were tested for their antibacterial properties *Klebsiella pneumoniae* and Multi Drug Resistant *Staphylococcus Aureus*. The antibacterial activity of the biosynthesized La_2O_3 NPs is mild.

++ PG & Research;

*Corresponding author: Email: alwindavid1986@gmail.com;

Cite as: Subramanian, P., and S. Alwin David. 2024. "Biosynthesis of La_2O_3 Nanoparticles Using *Lawsonia Inermis* Leaf Extract". UTTAR PRADESH JOURNAL OF ZOOLOGY 45 (18):161-69. <https://doi.org/10.56557/upjoz/2024/v45i184434>.

Keywords: La_2O_3 NPs; biosynthesis; *Lawsonia inermis*; antibacterial activity.

1. INTRODUCTION

North Africa, Australia, and Southwest Asia are popular places to cultivate *Lawsonia inermis*, a tropical and subtropical plant in the Lythracea family. To treat amoebic dysentery, the leaves are used internally. They are also used to encourage menstrual flow and cure diarrhea. They are applied topically to soothe sore throats. Because of the astringent properties of the leaf extracts, the skin becomes hydrophobic. It is a helpful medication for external use against various skin and nail ailments because of this effect as well as a minor antibacterial and fungicidal action.

For this reason, the leaves are applied externally to cure wounds, ulcers, herpes, and a variety of skin conditions, including leprosy. To make mouthwash, an infusion of the leaves is combined with salt and tobacco. Lice are successfully killed with henna hair dye.

Although a number of approaches have shown that lanthanum nanoparticles can be produced chemically and physically, the need to find an alternative method arises from the need to use a large quantity of costly reagents, hazardous chemicals, extended times, and high temperatures. The green chemistry approach highlights that using natural plants has provided an easy-to-use, dependable, safe, and environmentally friendly method [1-19].

2. MATERIALS AND METHODS

2.1 Chemicals Used

Lanthanum nitrate hexahydrate used for the synthesis of La_2O_3 NPs was purchased from nice chemicals. *Lawsonia inermis* leaves used in this work were collected from the local area (Thoothukudi, Tamil Nadu, India).

2.1.1 Preparation of *Lawsonia inermis* leaf extract

About 20g of fresh leaves of *Lawsonia inermis* were taken and washed thoroughly with distilled water to remove dust particles. These washed leaves were cut into very small pieces and boiled in 200 mL of distilled water for an hour in a round-bottom flask with a condenser. The leaf extract was filtered using Whatman

No. 41 filter paper to obtain the pure leaf extract.

2.1.2 Biosynthesis of La_2O_3 nanoparticles

About 50mL of freshly prepared *Lawsonia inermis* leaf extract was added to 100 mL of 0.1M $\text{La}(\text{NO}_3)_3 \cdot 6\text{H}_2\text{O}$ solution. This mixture was heated at 110°C for 1 hour. Then the synthesized La_2O_3 NPs were filtered, dried and calcined at 450°C for 2 hours.

2.1.3 Characterization

The JascoV-600 spectrophotometer was used to record the UV-visible spectra of the La_2O_3 NPs and the extract from *Lawsonia inermis* leaves. Thermo Scientific Nicolet iS5 FTIR spectrometer was used to measure FTIR. The average particle size of La_2O_3 NPs was determined by using XPERT-PRO X-ray diffractometer operating at a voltage of 40 kV and a current of 30 mA with Cu K α radiation. A TESCAN MIRA3 XMU device was used to conduct energy dispersive X-ray analysis (EDAX) and scanning electron microscopy (SEM).

3. RESULTS AND DISCUSSION

Characterizations and applications of La_2O_3 NPs are described below by various techniques. The results obtained are discussed in detail as follows:

3.1 UV-Vis Diffuse Reflectance Spectroscopy

An absorption band of *Lawsonia inermis* at 256 nm is due to the presence of benzene and quinone with $\pi-\pi^*$ electron transition. Another absorption band at 412 nm is due to the $n-\pi^*$ transitions of carbonyl group in the quinone ring [1].

UV-Visible spectroscopy is one of the most powerful techniques for characterizing nanoparticles and it provides information about the optical properties of nanoparticles.

Fig. 2. shows the UV-visible spectrum of green synthesized La_2O_3 NPs. The presence of sharp peaks at 245 nm can be attributed to valence band to conduction band transition in La_2O_3 . It confirms the formation of La_2O_3 NPs [2].

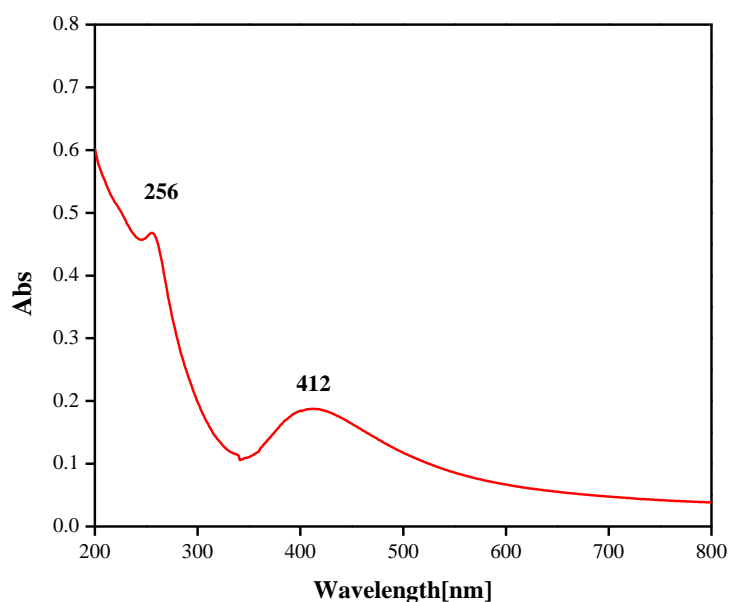


Fig. 1. UV-Vis spectrum of *Lawsonia inermis* leaf extract

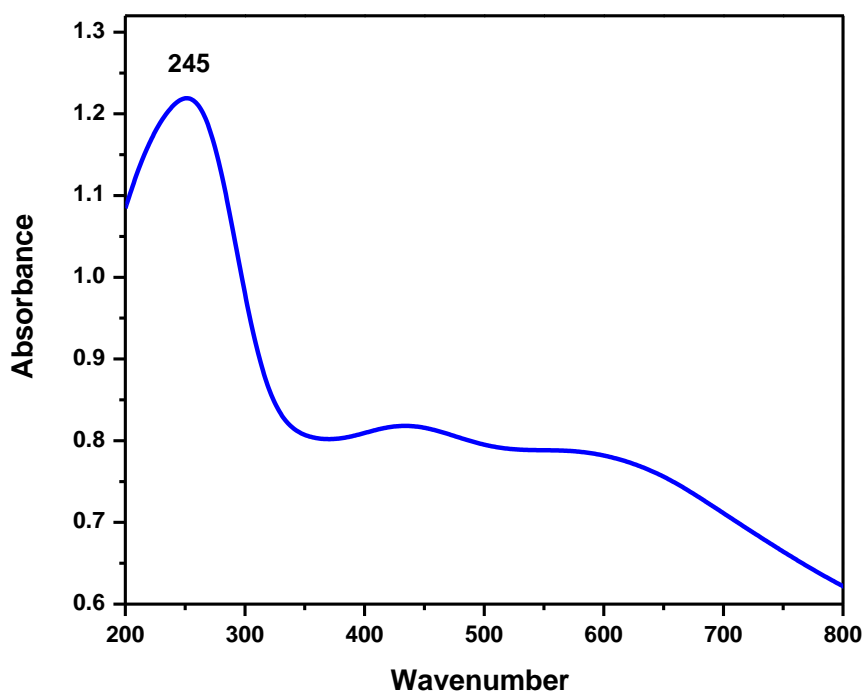


Fig. 2. UV-Visible diffuse reflectance spectrum of La₂O₃NPs

3.2 FTIR Analysis

A broadband centered at 3358 cm⁻¹ in Fig. 3 is attributed to the stretching vibration of the hydroxyl group which can be found at the first lawsone aromatic ring. The broad absorbance is due to the intramolecular hydrogen bonding between the OH group and adjacent oxygen atom. The adsorption band which appeared at

1634 cm⁻¹ is attributed to α , β -unsaturated carbonyl band. As seen in this IR spectrum, C=C is found as a weak band at 1384 cm⁻¹ signifying aromatic C=C group [3]. The band at 1042 cm⁻¹ is due to alkyl substituted ether [4] and C-N stretch in the sample. The peak observed at 567 cm⁻¹ belongs to the stretching of La-O, and this peak has demonstrated the formation of La₂O₃ NPs [5].

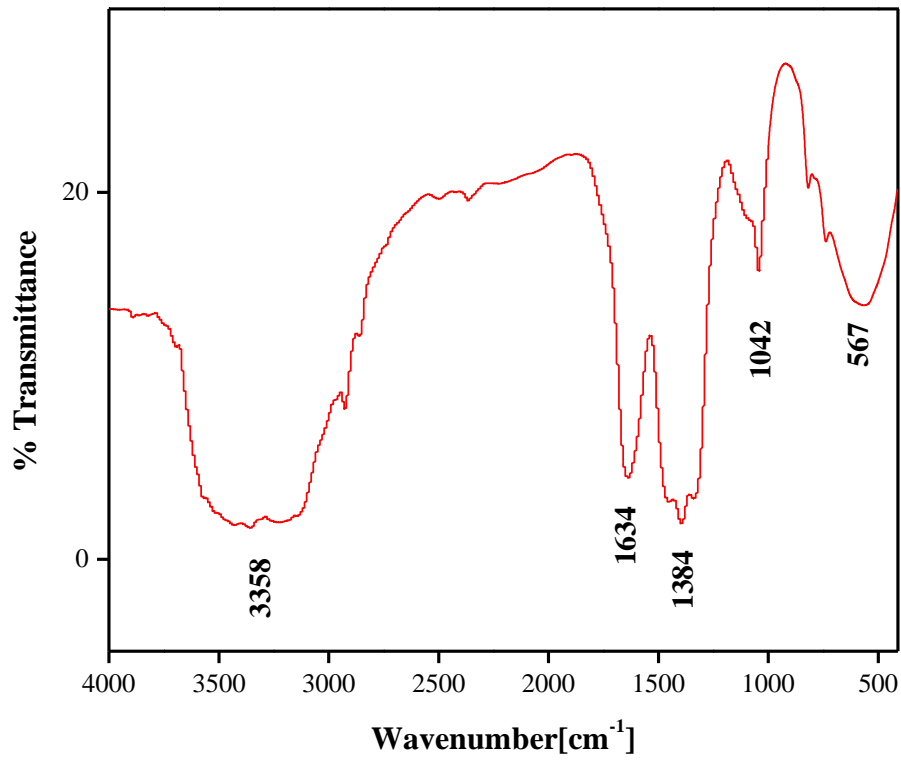


Fig. 3. FTIR spectrum of La₂O₃ NPs

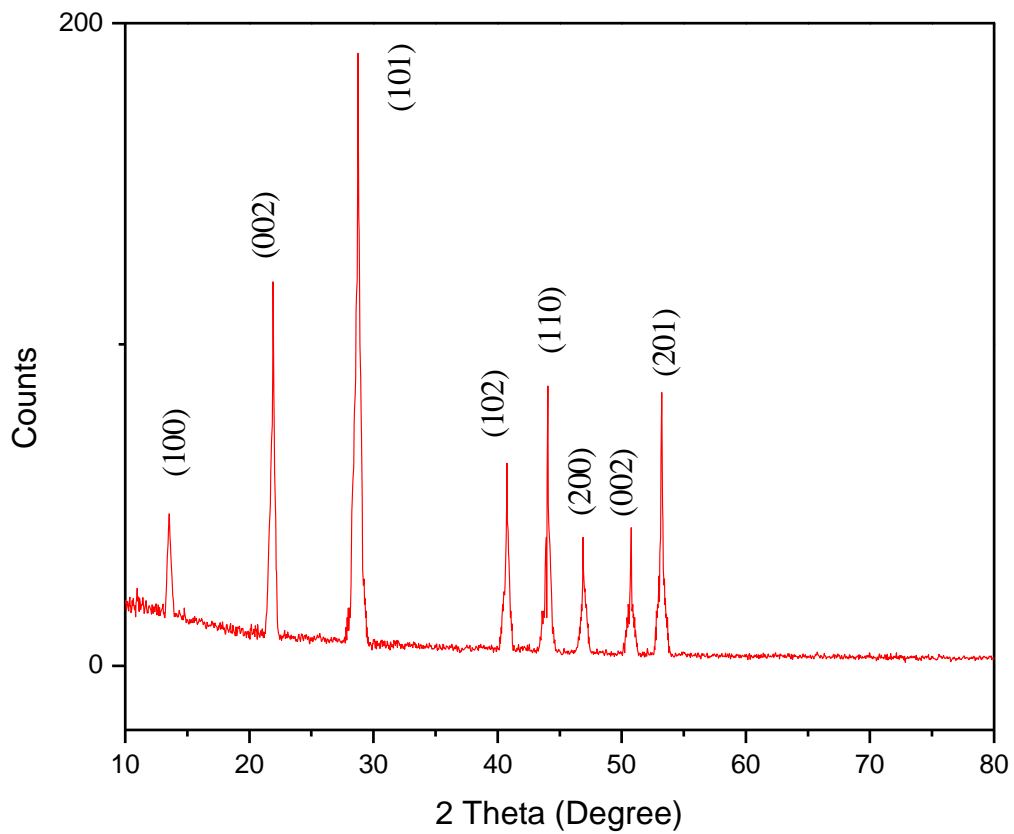


Fig. 4. XRD pattern of La₂O₃ NPs

3.3 X-ray Diffraction Analysis

The crystallite size can be evaluated using Debye-Scherer equation:

$$D = \frac{k \times \lambda}{\beta \cos \theta}$$

where D is the thickness (diameter) of the particle, λ is the wavelength of the X-ray beam, β is the full width at half maximum (FWHM) of the peak position in radians, k is the shape factor (0.9) and θ is the Bragg diffraction angle at peak position.

The analysis of XRD data using Debye-Scherer formula gives an average crystallite size of 24.99 nm. The crystallite size of the La₂O₃ NPs as estimated using the Scherrer formula is in the range of 14.67- 51.34nm.

The XRD peaks at 2θ values of 13.57°, 21.94°, 29.73°, 40.76°, 44.04°, 46.86°, 50.78° and 53.27° can be attributed to the (100), (002), (101), (102), (110), (200), (002) and (201)

crystalline planes of La₂O₃ NPs, respectively which matched with JCPDS No. 05–0602. XRD pattern (Fig. 4) thus clearly illustrates the formation of La₂O₃ NPs [6].

3.4 Field Emission Scanning Electron Microscopy (FESEM)

The FESEM reveals the surface morphology and approximate size of the La₂O₃ NPs. The FESEM images (Figs. 5-7) show that La₂O₃ NPs exhibit irregular shape. The size of the La₂O₃ NPs obtained from FESEM is in the range of 30 – 6 nm.

3.5 Energy Dispersive X - ray Analysis (EDAX)

Energy Dispersive X-ray analysis (EDAX) was done to determining the atomic contributions of the constituents in the nanoparticles. In the EDAX of La₂O₃ NPs (Fig. 8), La and O have weight (%) 84.05 and 15.95 respectively. The atomic (%) is found to be 37.77 and 62.23 for La and O, respectively.

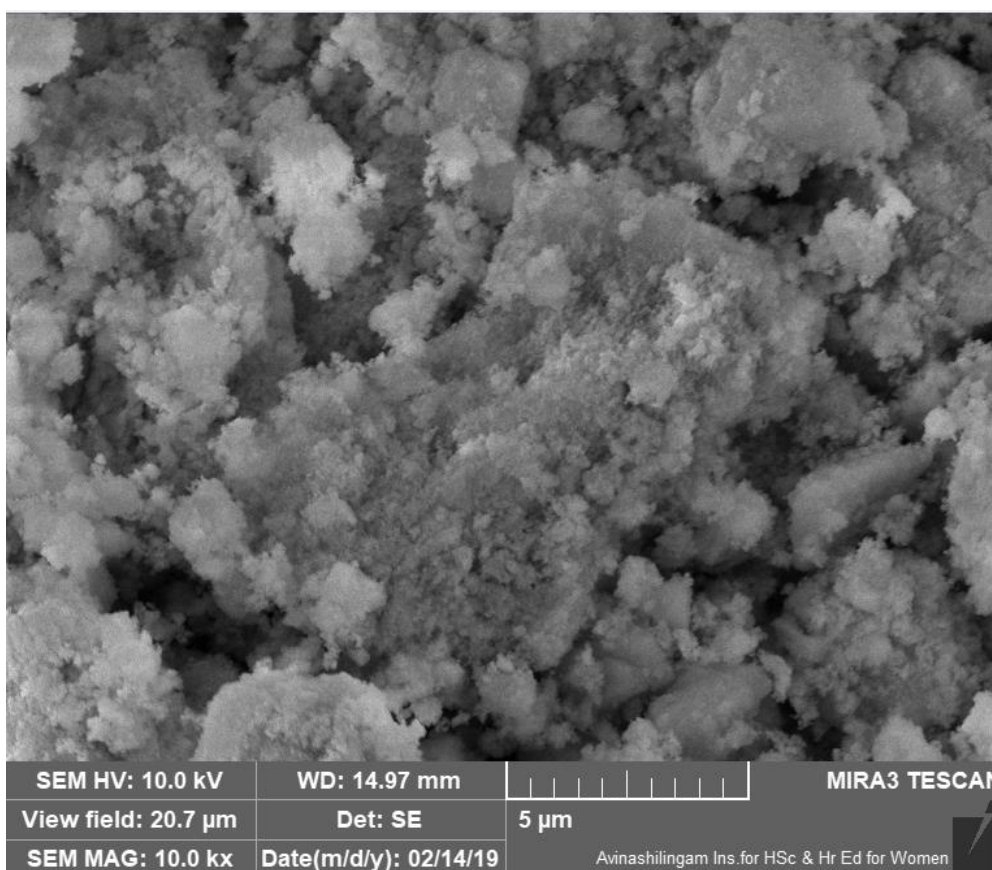


Fig. 5. FESEM image of La₂O₃ NPs in 5 μm scale

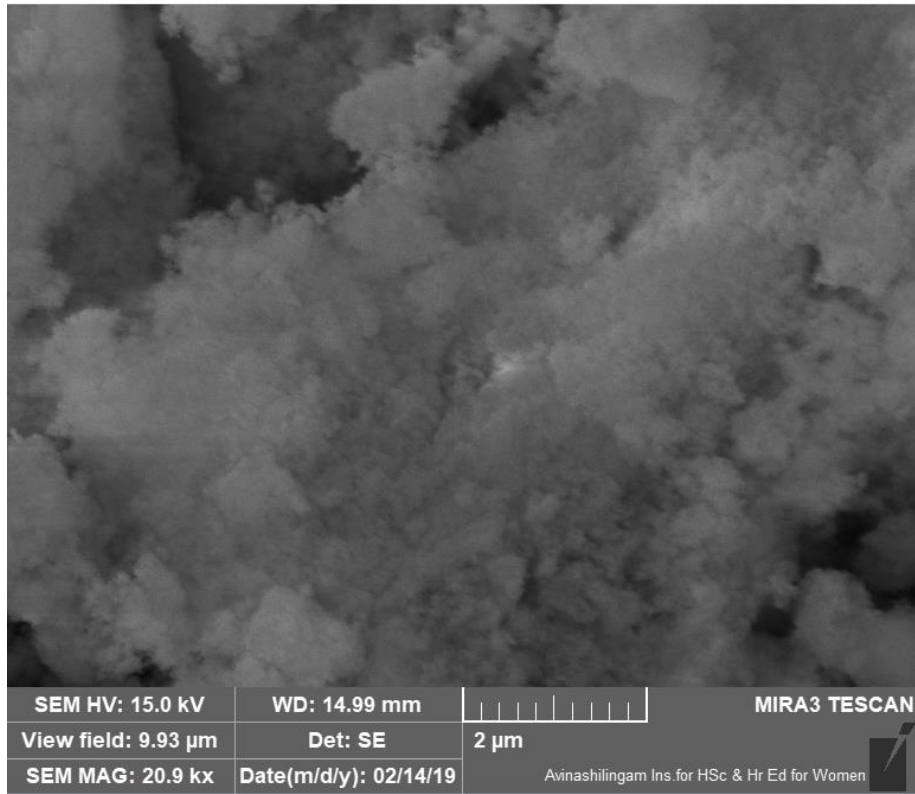


Fig. 6. FESEM image of La₂O₃ NPs in 2 μm scale

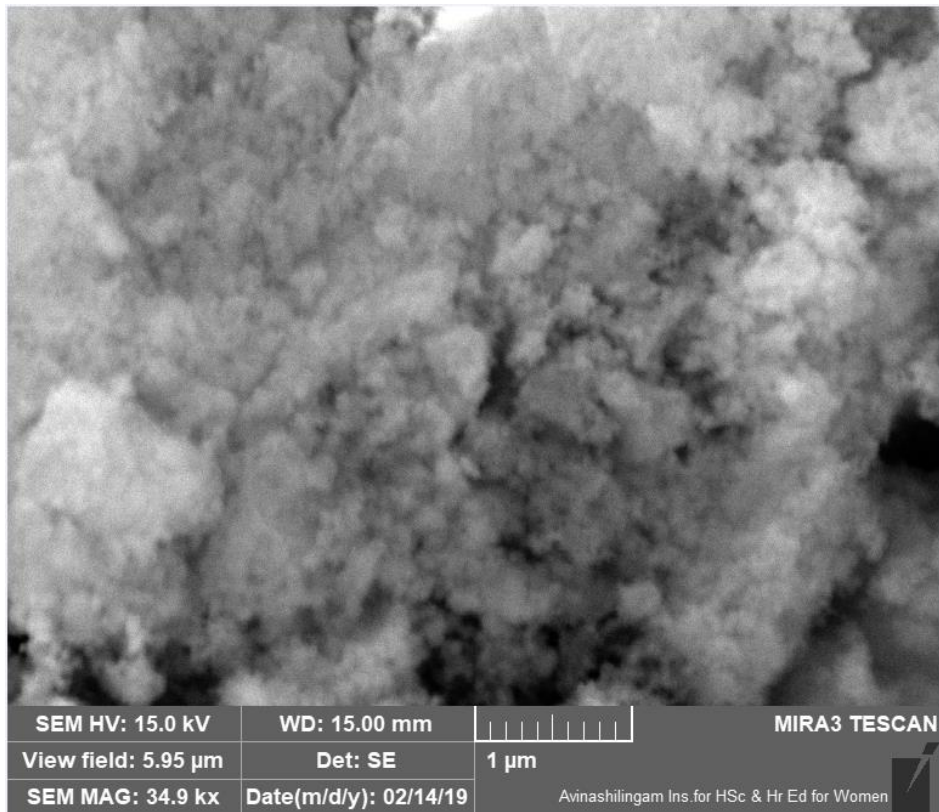


Fig. 7. FESEM image of La₂O₃ NPs in 1 μm scale

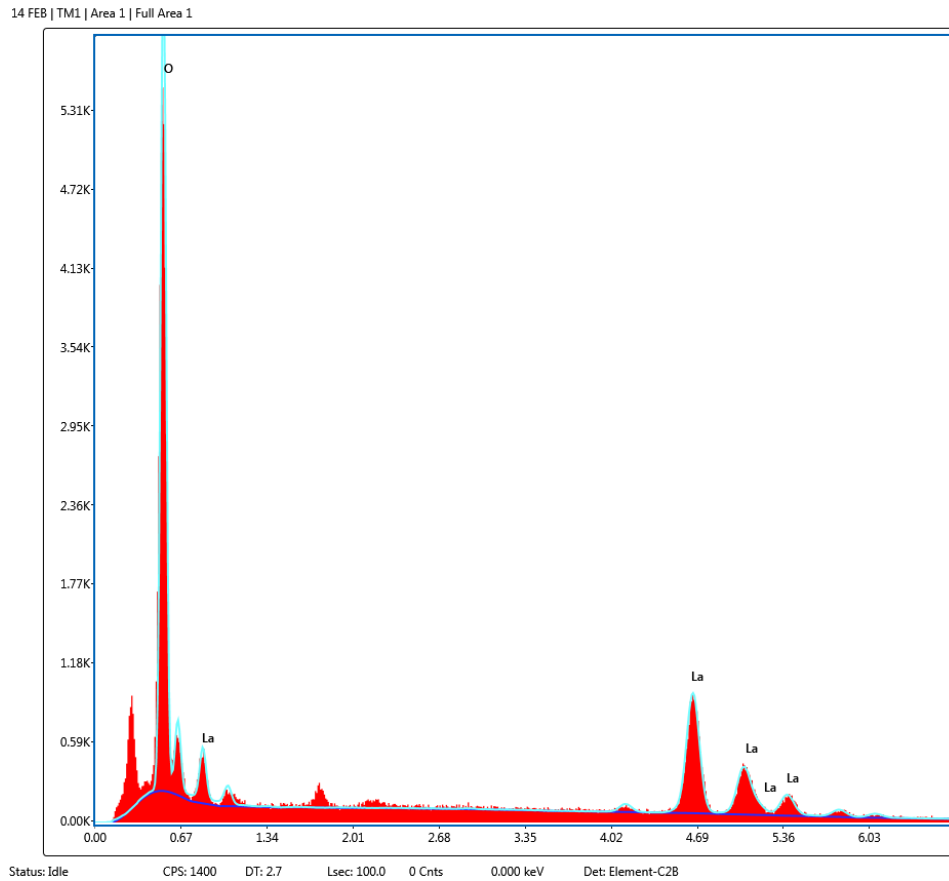


Fig. 8. EDAX spectrum of La_2O_3 NPs

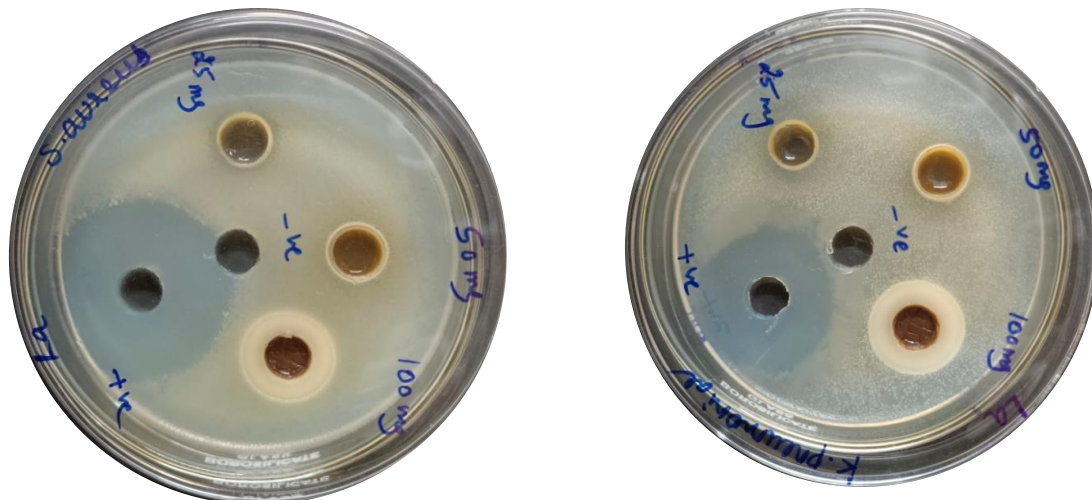


Fig. 9. Anti-bacterial activity of La_2O_3 NPs

Table 1. EDAX data of La_2O_3 NPs

Element	Weight %	Atomic %
La	84.05	37.77
O	15.95	62.23
Total	100.00	100.00

Table 2. Anti-bacterial Activity of Synthesized La₂O₃ NPs

Test Pathogens	Zone of Inhibition (ZOI) in mm				
	100 mg/mL	50 mg/mL	25 mg/mL	Positive Control	Negative Control
Multi Drug Resistant <i>Staphylococcus Aureus</i> (MRSA)	6	2	1	16	No ZOI
<i>Klebsiellapneumoniae</i>	7	2	1	13	No ZOI

Anti-bacterial activity was conducted against *Klebsiellapneumoniae* and Multi Drug Resistant *Staphylococcus aureus* (MRSA). The standard antibiotic chloramphenicol was selected as the comparison's control group (Positive Control). The antibacterial activity results demonstrated that all of the synthesized nanoparticles moderately inhibited both the bacterial strains of *Klebsiellapneumoniae* and Multi Drug Resistant *Staphylococcus Aureus*.

4. CONCLUSION

Bio synthesis of La₂O₃ NPs using the *Lawsonia inermis* leaf extract is demonstrated. The presence of sharp peaks at 245 nm in UV-Visible spectra confirm the formation of La₂O₃ NPs. Band at 567 cm⁻¹ in FT-IR spectra confirm the presence of La–O bond. La₂O₃ NPs have average particle size of 24.99 nm, as evidenced by XRD pattern. La₂O₃ NPs are found to be irregular in shape with variable size ranging from 30 to 60 nm, as evident by FESEM. EDAX confirms the presence of Lanthanum and Oxygen in the La₂O₃ NPs. The La₂O₃ NPs exhibit moderate antimicrobial activity against *Klebsiella pneumoniae* and Multi Drug Resistant *Staphylococcus Aureus*.

DISCLAIMER (ARTIFICIAL INTELLIGENCE)

Author(s) hereby declare that NO generative AI technologies such as Large Language Models (ChatGPT, COPILOT, etc) and text-to-image generators have been used during writing or editing of manuscripts.

COMPETING INTERESTS

Authors have declared that no competing interests exist.

REFERENCES

1. Fernandez A, George A, Remadevi VK. Synthesis, characterization, antioxidant, DNA cleavage and cytotoxic studies of amino derivatives of lawsone. International Journal of Phytopharmacy. 2013;1:36–41.
2. Abazari R, Sanati S, Saghatforoush LA. A unique and facile preparation of lanthanum ferrite nanoparticles in emulsion nanoreactors: Morphology, structure, and efficient photocatalysis. Materials Science in Semiconductor Processing. 2014;25: 301–306.
3. Zulkifli F, Ali N, Yusof MSM, Khairul WM, Rahamathullah R, Isa MIN, Wan Nik WB. The effect of concentration of Lawsonia inermis as a Corrosion Inhibitor for Aluminum Alloy in Seawater. Advances in Physical Chemistry. 2017;1–12.
4. Hassan Wagini N. Phytochemical Analysis of Nigerian and Egyptian Henna (*Lawsonia Inermis* L.) Leaves using TLC, FTIR and GCMS. Plant. 2014;2(3):27.
5. Khalaf WM, Al-Mashhadani MH. Synthesis and characterization of lanthanum oxide La₂O₃ Net-like nanoparticles by new combustion method. Biointerface Research in Applied Chemistry. 2021;12(3):3066–3075.
6. Basavaraju N, Prashantha SC, Nagabhushana H, Naveen Kumar A, Chandrasekhar M, Shashi Shekhar TR, Ravikumar CR, Anil Kumar MR, Surendra BS, Nagaswarupa HP. Luminescent and thermal properties of novel orange–red emitting MgNb₂O₆: sm³⁺ phosphors for displays, photo catalytic and sensor applications. SN Appl. Sci. 2021;3:1–15.
7. Alwin David S, Vedhi C. Synthesis and characterization of Co₃O₄ - CuO - ZrO₂ ternary nanoparticles. International Journal of Chem Tech Research. 2017;10:905 – 912.
8. Alwin David S, Vedhi C. Synthesis, characterization and photocatalytic activities of Co₃O₄- MnO₂ - ZnO Ternary Nanoparticles. ECS Transactions. 2022; 107:2003,
9. S. Alwin David, V. Veeraputhiran and C. Vedhi, Spectroscopic and Morphological Behavior of Co₃O₄-MnO₂-ZrO₂ Ternary

- Nanoparticles. Journal of Nanoscience and Technology. 2017;3(4):296–298.
10. Alwin David S, Vedhi C. Synthesis of nano Co_3O_4 - MnO_2 - ZrO_2 mixed oxides for visible-light photocatalytic activity. International Journal of Advance Research in Science and Engineering. 2017;6(01): 613-623.
 11. Alwin David S, Subramanian P. Antibacterial activity of CuO nanoparticles synthesized by *Justicia Adhatoda* leaf extract. Journal of Pharmaceutical Research International. 2021;33(56B): 160-170.
 12. Mohammad Mahdi Najafpour, Fahimeh Rahimi, Eva-Mari Aro, Choon-Hwan Lee and Suleyman, Allakhverdiev I. Nano-sized manganese oxides as biomimetic catalysts for water oxidation in artificial photosynthesis: A review. J. R. Soc. Interface. 2012;9(75):2383-2395.
 13. Alwin David S, Rajadurai SI, Kumar SV. Biosynthesis of copper oxide nanoparticles using *Momordica charantia* leaf extract and their characterization. International Journal of Advance Research in Science and Engineering. 2017;6(03):313-320.
 14. Alwin David S, Revathi LU. Green synthesis of Fe_3O_4 nano particles using *Camellia angustifolia* leaf extract and their enhanced visible-light photocatalytic activity. International Journal of Advance Research in Science and Engineering. 2018;7(02):422- 428.
 15. Jinge Li, Pengyi Zhang, Jinlong Wang, Mingxiao Wang, Birnessite-type manganese oxide on granular activated carbon for formaldehyde removal at room temperature. The Journal of Physical Chemistry C. 2016;120(42):24121 -24129.
 16. Alwin David S, Subramanian P. Biogenesis of zirconium oxide nanoparticles by *Momordica charantia* (Bitter Gourd) leaf extract: Characterization and their antimicrobial activities. Journal of Pharmaceutical Research International. 2021;33(61B):354-362.
 17. Alwin David S, Ram Kumar. Biogenesis of MnO_2 nanoparticles using *Momordica Charantia* leaf Extract. ECS Transactions. 2022;107:747.
 18. Subramanian P, Alwin David S. *Momordica charantia* leaf extract mediated zinc oxide nanoparticles for antibacterial performance. Uttar Pradesh Journal of Zoology. 2024;45(12): 179–188.
 19. Subramanian P, Alwin David S. Antibacterial activity of *Piper Betle* leaf extract mediated MnO_2 nanoparticles. Uttar Pradesh Journal of Zoology. 2024;45(14): 245-52.

Disclaimer/Publisher's Note: The statements, opinions and data contained in all publications are solely those of the individual author(s) and contributor(s) and not of the publisher and/or the editor(s). This publisher and/or the editor(s) disclaim responsibility for any injury to people or property resulting from any ideas, methods, instructions or products referred to in the content.

© Copyright (2024): Author(s). The licensee is the journal publisher. This is an Open Access article distributed under the terms of the Creative Commons Attribution License (<http://creativecommons.org/licenses/by/4.0>), which permits unrestricted use, distribution, and reproduction in any medium, provided the original work is properly cited.

Peer-review history:

The peer review history for this paper can be accessed here:

<https://prh.mbimph.com/review-history/3970>